doi:10.1017/S1431927622003464
Microsc. Microanal. 28 (Suppl 1), 2022

Expanding the Limits of Atom Probe Crystallographic Analysis

Andrew J. Breen[1], Alec C. Day[1], Felix Theska[2], Bryan Lim[1], William Davids[1], Sophie Primig[2] and Simon P. Ringer[1]

[1.] School of Aerospace, Mechanical and Mechatronic Engineering, and Australian Centre for Microscopy and Microanalysis, The University of Sydney, Sydney, NSW, Australia
[2.] School of Materials Science and Engineering, UNSW, Sydney, NSW, Australia
* Corresponding author: simon.ringer@sydney.edu.au

The crystallographic information contained within atom probe tomography (APT) datasets of crystalline specimens is useful for a variety of reasons. It can facilitate calibration of the tomographic reconstruction [1] as well as enable direct crystallographic measurements of microstructural features such as grain boundaries [2] or site occupancy behavior in ordered phases at the atomic scale. The results of these types of crystallographic analysis methods are often of particular interest to better understand structure-property-processing relationships in engineering materials.

Crystallographic information within APT datasets has traditionally been accessed through interrogation of the density variations in the field evaporation image (FEI) in the form of poles and zone lines as well as through reconstructed lattice planes within the corresponding tomographic reconstruction [3]. However, this information is highly dependent on material properties and experimental parameter selection and not always trivial to observe. Voltage pulsing and low specimen temperatures usually promotes improved crystallographic signal within the data, however this is often at the expense of lower experiment success rates. Significant scope exists to improve existing crystallographic analysis methods so that they are applicable to a wider scope of materials and experimental parameters and provide improved quantitative information on crystallography related phenomena. Recent APT hardware developments such as the increased field of view (FoV) and dual deep UV laser pulsing on the newly launched CAMECA Invizo 6000 [4] also offer exciting opportunities to extend APT crystallographic analysis.

This study looks at new developments in sophisticated APT crystallographic analysis approaches and the opportunities to extend these methods on the CAMECA Invizo 6000 platform. A range of industrially significant engineering materials were selected to showcase the developed analysis approaches including electron powder bed fusion (E-PBF) produced Ni-based superalloy Inconel 738 (IN738). APT blanks were cut from different regions of the IN738 builds and electropolished before being analyzed in the CAMECA LEAP 4000 X Si and CAMECA Invizo 6000. The datasets were then exported as .epos files from AP suite 6 and imported into Matlab for improved bespoke crystallographic analysis. A range of crystallographically correlated metrics were then identified to enhance the observation of poles and zone lines in the detector space to facilitate pole indexing and accurate crystallographic calibration of the reconstructions. The $L1_2$ ordered γ' phase in IN738 was of particular interest as it is the major strengthening phase of this alloy. A detailed quantitative analysis of the site-occupancy behavior of added substitutional solute additions was then performed using a new method based on Gaussian curve fitting of species specific spatial distribution maps (SDMs).

Figure 1 is a collection of different detector mapping approaches for 2 million sequential ions from a primary γ' region contained within an APT dataset of IN738 collected on the LEAP 4000 X Si. In the

raw FEI (Figure 1a), limited crystallographic information can be observed in the form of low density poles. In Figure 1b, the FEI has been filtered for 0 < the number of pulses between detection events (nulls) < 10 and proves effective at highlighting zone lines not readily apparent in the raw FEI. Figure 1c is a corresponding detector map displaying the average distance squared between +/- 2 sequential ion detection events for each bin across the detector space and further reveals additional crystallographic information including higher index poles not readily apparent in the raw FEI. Figure 1d contains the corresponding stereographic projection of the crystal, pole indexing and unit cell orientation based on the information obtained from the various detector hit maps.

Figure 2a is a representative calibrated reconstruction of IN738 showing γ and γ' regions. Figure 2b is a zoomed in region of interest (ROI) around the 002 pole revealing the ordered nature of reconstructed lattice planes in γ'. Figure 2c are the corresponding species-specific spatial distribution maps (SDMs) [3] of Ni and a selection of substitutional solute species. By comparing the different SDM responses, the site preferencing behavior of the elements to the alpha (unit cell faces) or beta (unit cell corners) can be deduced. By further fitting the central major and minor peaks of the SDMs to a bimodal Gaussian distribution, the relative fraction that a species substitutes for the alpha or beta sites can be quantified. It was found that the relative alpha/beta site occupancy ratio of some mixed occupancy elements such as Co changed throughout the build height and could be a contributing factor to corresponding changes in the elastic properties of the build [5].

The results demonstrate that latent crystallographic information can be contained within APT datasets of crystalline materials such as In738. Different data metrics accessible through the .epos file can be used for an holistic approach to detector mapping to reveal information not readily apparent in the raw FEI. Such information is useful for accurate calibration of the reconstruction and performing crystallographic measurements such as site-occupancy quantification in intermetallics including $L1_2$ ordered IN738. Results will also be compared to new data currently being acquired on the CAMECA Invizo 6000 and the implications of a larger FoV and dual deep UV pulsing in the context of APT crystallographic analysis will be discussed.

References:

[1] AC Day et al., Microscopy and Microanalysis **25** (2019), p. 288–300. doi:10.1017/S1431927618015593.
[2] AJ Breen et al., Microscopy and Microanalysis **23** (2017), p. 279–290. doi:10.1017/S1431927616012605
[3] MP Moody et al., Ultramicroscopy **109** (2009), p. 815–824. doi:10.1016/j.ultramic.2009.03.016.
[4] Invizo 6000 - 3D Atom Probe, https://www.cameca.com/products/apt/invizo-6000 (accessed February 10, 2022).
[5] B Lim et al., Additive Manufacturing **46** (2021), p. 102121. doi:10.1016/j.addma.2021.102121

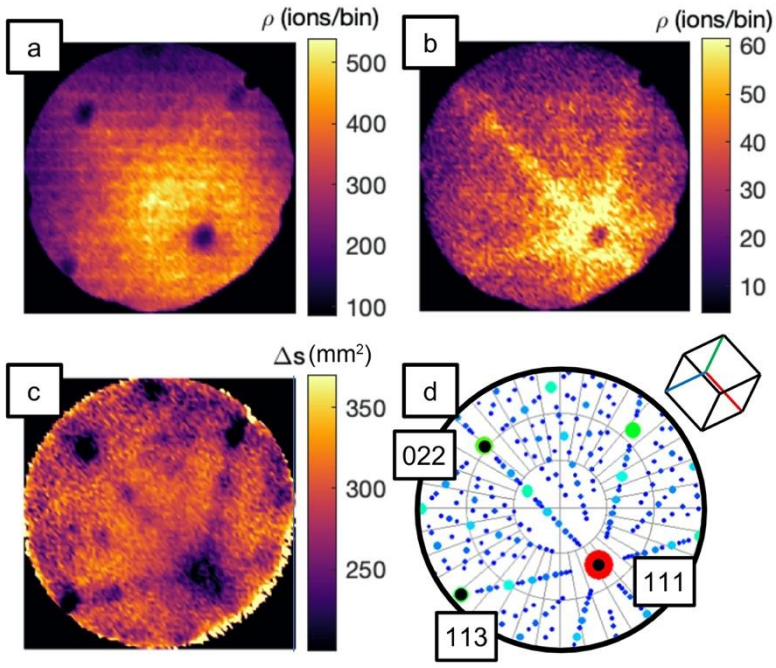

Figure 1. a) FEI of 2 million sequential ions from the γ′ phase in E-PBF produced In738. b) FEI filtered for 0 < nulls < 10. c) Corresponding detector map of distance between successive evaporation events. d) Corresponding stereographic projection with pole indexing and unit cell orientation.

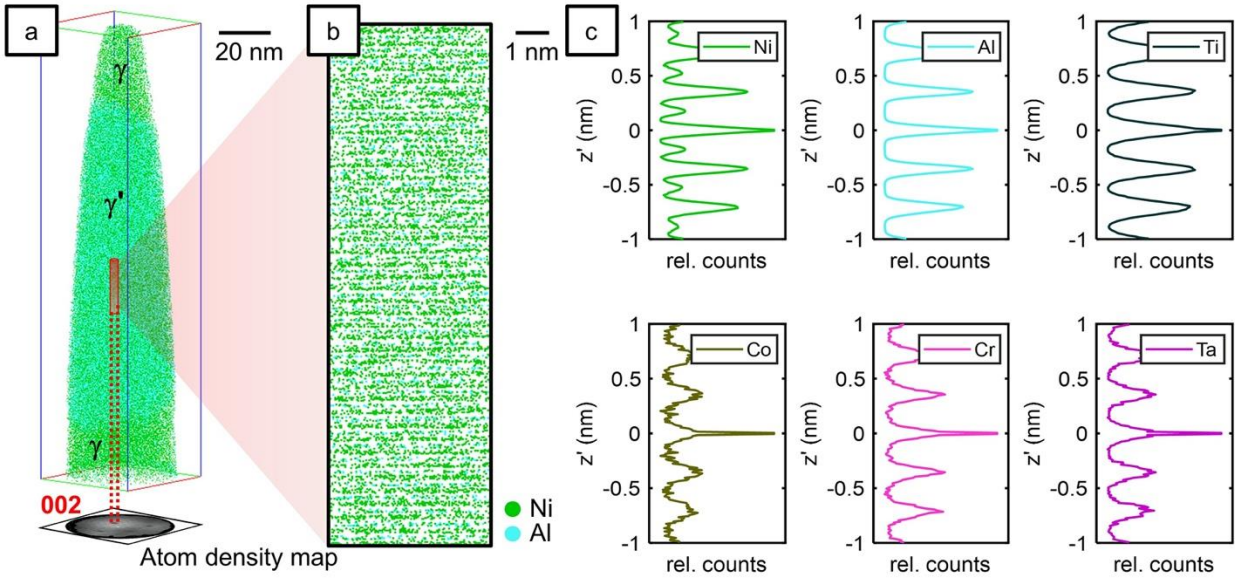

Figure 2. a) APT reconstruction of E-PBF IN738 showing γ and γ′ regions with corresponding atom density map used to locate the 002 pole region. b) zoomed in region of interest around the 002 pole in γ′ showing reconstructed ordered lattice planes. c) species-specific spatial distribution maps of some of the substitutional solute additions that can be used to determine site occupancy behavior.

https://doi.org/10.1017/S1431927622003464 Published online by Cambridge University Press